TITANIUM EUROPE 2015 - International Titanium Association May 11-13, 2015
Hilton Birmingham Metropole Hotel, Birmingham, UK

Manufacture of Complex Titanium Parts using Wire+Arc Additive Manufacture

Adrian Addison, Jialuo Ding, Filomeno Martina, Helen Lockett, Stewart Williams
Welding Engineering and Laser Processing Centre (WELPC), Cranfield University, Cranfield, MK43 0AL, United Kingdom
Xiang Zhang, Faculty of Engineering and Computing, Coventry University, Coventry CV1 2JH, UK

Abstract
Wire+arc additive manufacture (WAAM) for titanium is a process which is gaining interest in several industry sectors due to its capability to produce parts of medium to high complexity in medium to large scale, without the need for large complex tooling the process uses relatively simple and readily available welding equipment and manipulators. In the case of titanium, the process produces deposits with acceptable, though isotropic mechanical properties which can be further improved through the introduction of cold working processes which cause predictable refinement of the microstructure an improvement of the related mechanical properties which then become anisotropic. This paper provides a review of achievable mechanical properties for Ti-6Al-4V, before the process of using WAAM to manufacture some medium complexity demonstration parts is described.

1. Introduction
Wire+arc additive manufacture (WAAM) for titanium is a process which is gaining interest in several industry sectors due to its capability to produce near-net-shape preforms for parts of medium to high complexity in medium to large scale without the need for large, complex tooling using relatively simple and readily available welding equipment and manipulators. In the case of titanium, the process produces deposits with acceptable, though isotropic mechanical properties (1) which can be further improved through the introduction of cold working processes which cause predictable refinement of the microstructure and improvement of the related mechanical properties which then become anisotropic (3).

Although the essence of the WAAM process was described in Baker's 1926 patent "The use of an electric arc as a heat source to generate 3D objects by depositing molten metal in superimposed layers" it was not seriously examined for manufacture of 2.5D components in titanium alloys at Cranfield University until 2007, when TiG and plasma transferred arcs were used as a heat source (2).

It is unfortunate that many of the additive manufacturing processes for metallic materials are often considered as a group of processes with similar capabilities, competing for the same applications. However, this is not the case as every process has a set of capabilities which is identifiable, but may overlap other processes slightly. For example, laser beam and powder processes offer advantages of high process resolution, design freedom, topological optimisation and net shape part production, but are limited by the physical restraints on equipment size, deposition rates of a few hundred grams per hour and the requirement for hot isostatic pressing. This has led to some production applications where the advantages outweigh the disadvantages.

The deposition rate of WAAM for titanium alloys is between 0.75 and 2kg/hour with a process resolution and surface waviness (or macro roughness) in the order of 0.5mm. The deposits are fully dense, do not require HIPing and are limited in size only by the reach of the manipulator in use. So, when compared to laser powder based and other AM processes, WAAM has a different set of capabilities and a correspondingly different set of advantages and disadvantages.

The type of part that WAAM is most capable of manufacturing is in a medium to large scale >400mm and of medium complexity. In the aerospace industry, there are entire families of this type of part for which the most common manufacturing methods are subtractive, machining from either solid billet or forgings with a very high buy to fly ratio. Consultation with aerospace OEMs has suggested that WAAM could be used to provide an alternative manufacturing method for this type of part, where a near-net-shape pre-form with an envelope of at least 1.0mm on each surface for final machining to ensure both accuracy and surface finish requirements would reduce buy to fly ratio, reduce the reliance on large forgings and therefore give benefits in both cost and lead time. As a result, there is a desire to mature the process for adoption into mass production for class 1 aerospace components.

As the production of relatively simple walls from which test samples could be extracted progressed and favourable property values emerged, the need to provide “technology demonstrator” parts of increasingly complex geometry has led to generation of a volume of knowledge relating to the build of these parts. This knowledge is being captured in theses, papers (4), presentations and prototype computer software produced by the maturation programme (WAAMMat) being run by Cranfield University.

2. As Deposited Mechanical Properties

This section contains extracts from previously published work (1) and is paraphrased here for reference. The original work should be consulted for details.

2.1 Microstructure

Ti-6Al-4V wire was deposited layer by layer onto a substrate in a single bead without weaving. For each successive layer, the deposition direction was reversed. Two straight walls, both 6.8 mm in thickness, were produced - Build 1 was 925mm long and 195mm high, while Build 2 was 975mm long and 155mm high.

Figure 1(a) shows a typical macrostructure of the as-deposited Ti-6Al-4V alloy. The vertical light and shaded stripes are columnar prior-b grains that developed during solidification and grew from the substrate across the deposited layers. They extended to the top of the sample and had an average grain width of 1 to 2 mm. The colour variation in the columnar grains is caused by their different crystallographic orientations. The preferred growth direction of the prior-b columnar grains was almost perpendicular to the substrate.

The upper unbanded region at the top of the wall consisted of martensitic a’ near the top surface, which progressively changed to a very fine Widmenstatten α microstructure moving down toward the first band as shown in Figure 1(b). In contrast, below the top five layers in the majority of the wall, there was a transition across each band, where the microstructure graduated from a finer to a coarse lamellar a Widmenstatten structure, as shown in Figure 1(c)–(d), and the white bands coincided with the coarsest lamellar plate width, Figure 1(d).

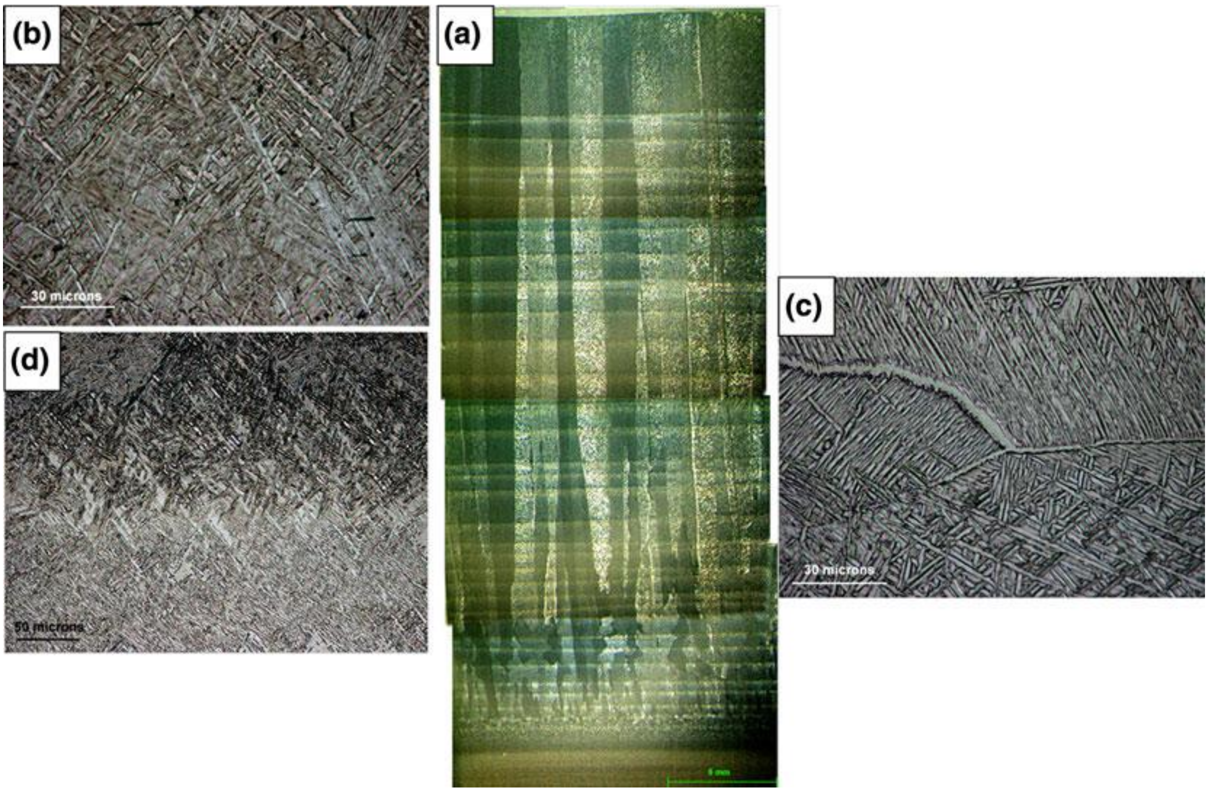

Figure 1. Optical macrostructure and microstructure of the as-deposited Ti-6Al-4V:
(a) macrostructure showing columnar β grains and macroscopic white bands;
(b) microstructure from the top layer of the build region showing a fine α’ morphology;
(c) typical microstructure of the majority of the wall between the bands showing a coarser Widmenstatten structure;
(d) Microstructure between two neighbouring bands showing a transition from a coarse to a fine Widmenstatten structure.

2.2 Tensile Performance

Test samples were extracted from the previously described wills in both the horizontal (parallel to the layers) and vertical (perpendicular to the layers) as shown in figure 2. The test samples were extracted and tested according to ASTM-E8-04.

The tensile test results are summarized in Figure 3. Baseline specimens from a forged Ti-6Al-4V bar, which had a duplex microstructure, are also shown for comparison purposes. No systematic correlation was found between the position of a sample within the wall and its tensile test results. However, there was a significant effect of sample orientation. The average yield strength (YS), ultimate tensile strength (UTS), and strain to failure from the baseline tests were 950 MPa, 1033 MPa, and 11.7%, respectively. In comparison, the samples tested from the vertical build direction exhibited a lower strength, with a mean yield strength of 803 MPa and UTS of 918 MPa. The tensile strength properties were, therefore, only moderately anisotropic.

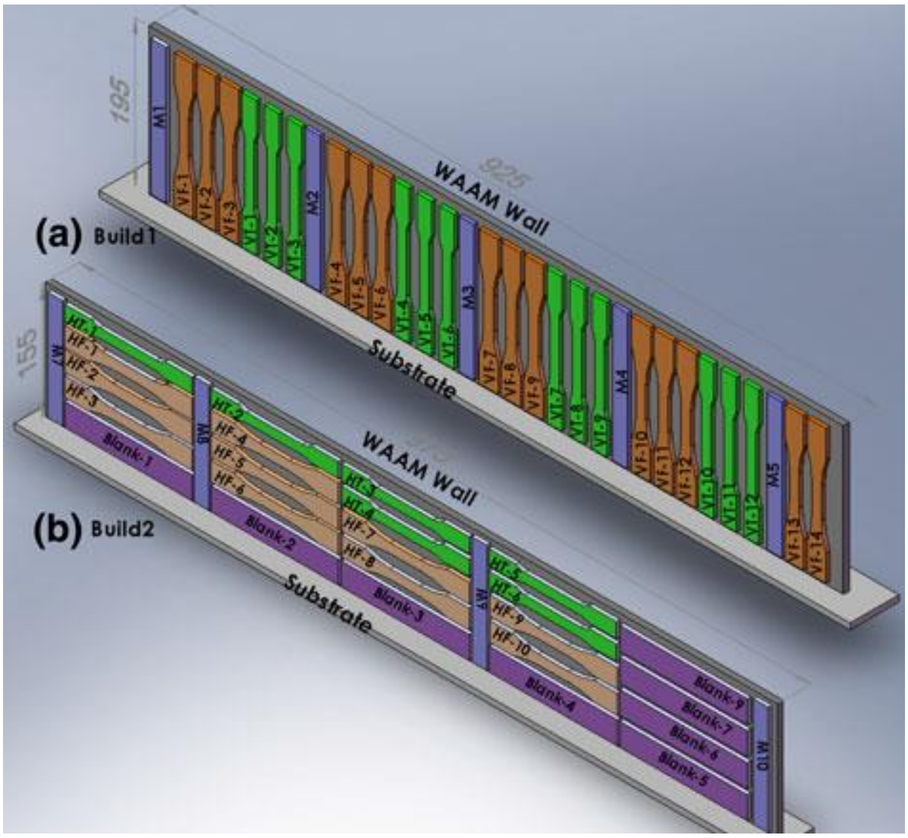

Figure 2. Illustration of tensile test samples within WAAM walls

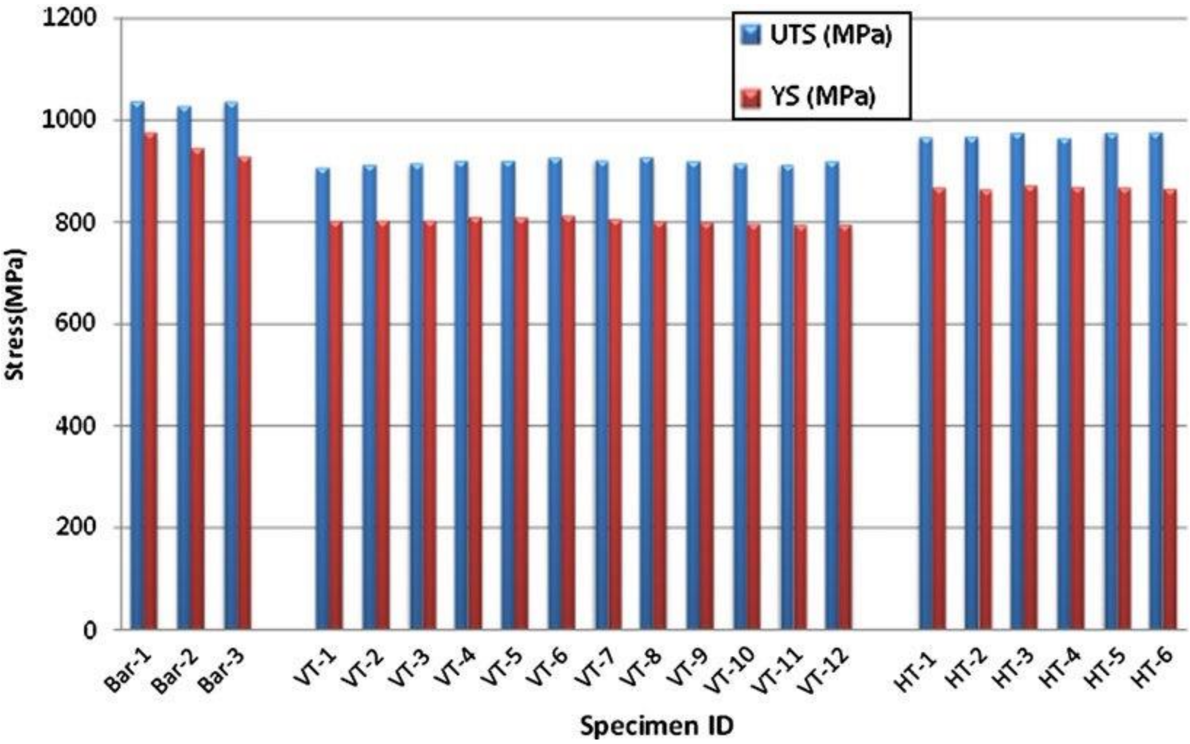

Figure 3. Tensile test results for WAAM of Ti-6Al-4V

2.3 Fatigue Properties

The fatigue results from the thirty-six ALM samples and five baseline specimens are summarized in Figure 4. The three baseline specimens failed well below one million cycles with the remaining two failing at just over one million cycles. Sixteen of the as-deposited specimens did not fail after ten million (107) cycles when the test was stopped. In total, twenty-one samples had a fatigue life well above three million cycles. However, there were still three samples where failure occurred below one million cycles, as indicated by the arrows in the figure. With the limited dataset tested, no statistically valid relationship could be demonstrated between a specimen's orientation and location (see Figure 2) and its fatigue life. However, of the few specimens that failed below one million cycles, two were orientated horizontally within the wall and the vertical sample that failed prematurely was machined from close to the wall end. Comparing the fatigue test results of the WAAM Ti-6Al-4V samples to the baseline bar specimens shows that the average high-cycle fatigue resistance of WAAM specimens, at this load level, was significantly better than that of the baseline bar specimens.

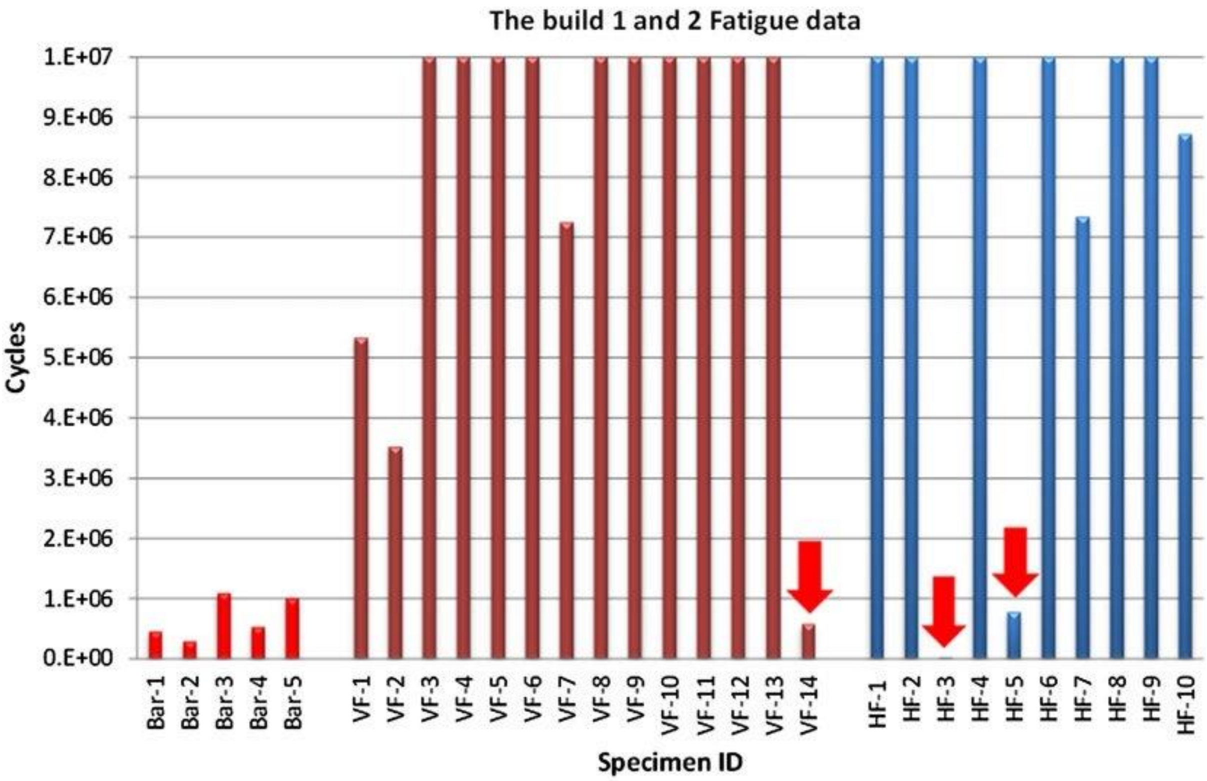

Figure 4. Fatigue test cycles to failure vs specimen ID. Note that a value of 10^7 indicates that a run-out occurred

2.4 Fracture Toughness Testing

The details of this testing are reported (5) and due for further publication in 2015, only the objective results are summarised here. To allow a direct comparison between standard and low oxygen content wire and parallel and oscillated bead methodologies, three WAAM walls measuring 50mm long, 100mm tall and 22mm wide were manufactured; the first using standard Ti-6Al-4V wire to AMS 4954 with a parallel bead build method, the second with the same wire but an oscillated bead build method and a third using low oxygen ELI Ti-6Al-4V alloy wire to AMS 4956 and a parallel bead build method. Each was sufficient to allow extraction of two specimens each in the L-T and T-L directions as shown in figure 5.

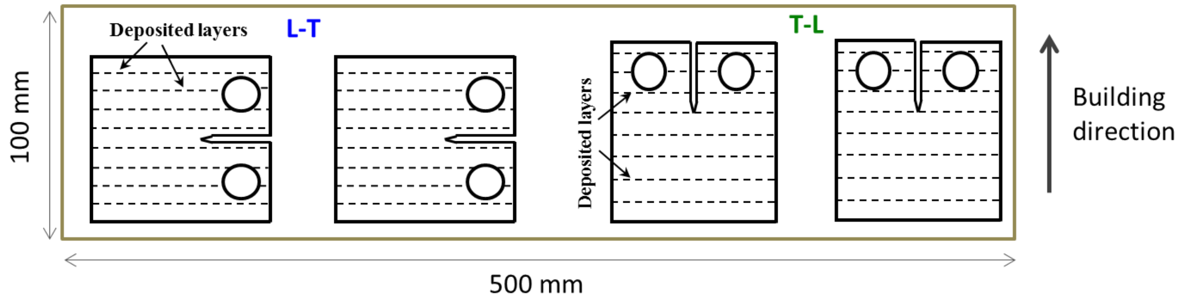

Figure 5. Layout of specimens within WAAM wall.

The specimens were manufactured and tested in accordance with ASTM 399, with the exception that the specimen thickness was limited to 19mm by the maximum load of the testing machine available. Since this would result in an "apparent" K_{1c} value, a sample of wrought Ti-6Al-4V (AMS 4911) was also prepared to allow a direct comparison to be made.

The results of the testing are shown in figure 6

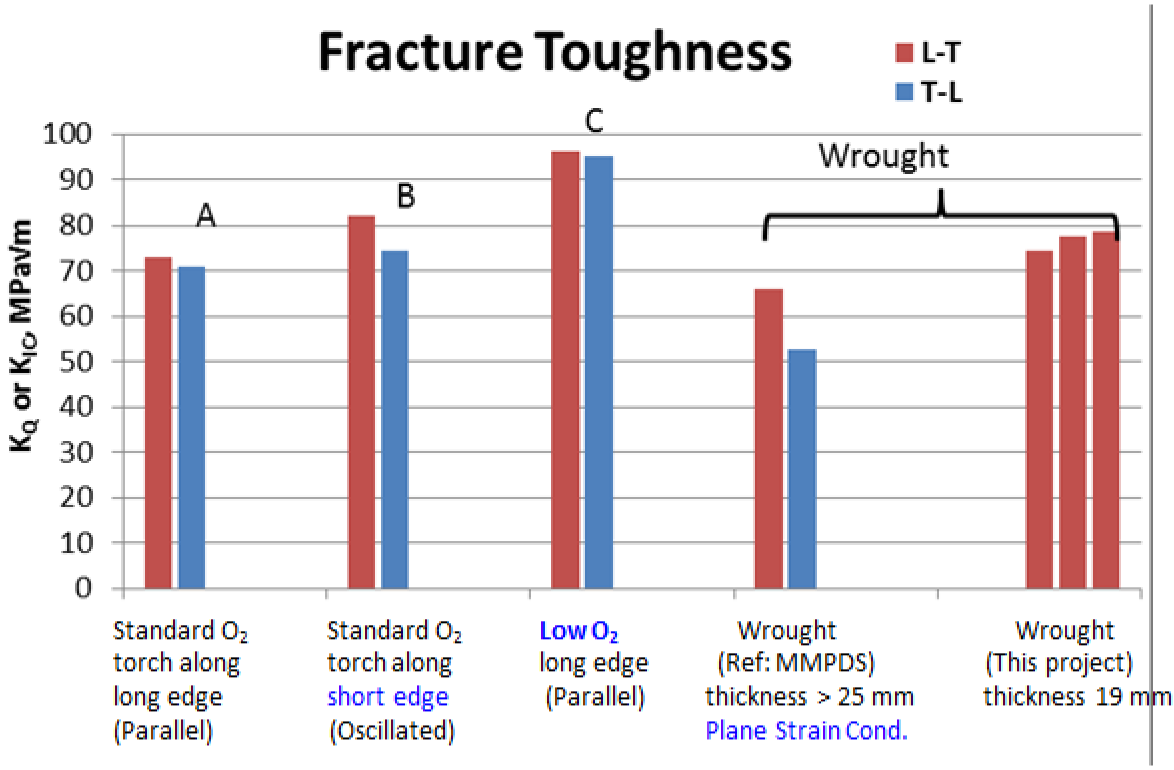

Figure 6. Apparent K_{1C} values for as-deposited Ti-6Al-4V WAAM

2.5 Crack propagation at WAAM to Wrought Interface

Again, the details of this testing are reported (6) and due for further publication in 2015, but the objective and results are summarised here. The aim of the study was to examine the fatigue crack growth rate and trajectory on and around the area of an interface between wrought and WAAM Ti-6Al-4V. A sample consisting of a Ti-6AL-4V to AMS 4911 plate, 450mm long, 60mm wide and 8mm thick, with a single bead width WAAM wall 8mm thick and 60mm tall built onto one edge. This sample allowed the extraction of test specimens to ASTM E647-13 in five different orientations as shown in figure 7.

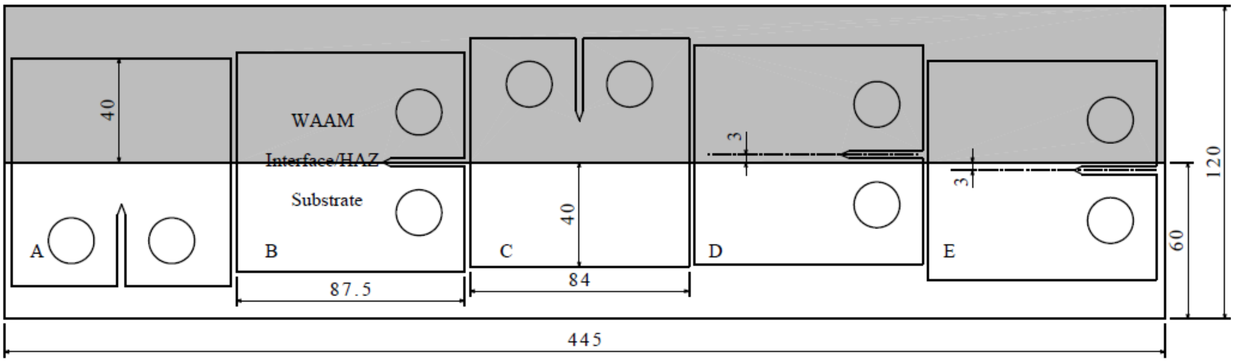

Figure 7. WAAM sample for crack growth sample extraction

The results of the test are summarised in figure 8 and indicate that the crack growth rate of the WAAM material is lower than that of the wrought.

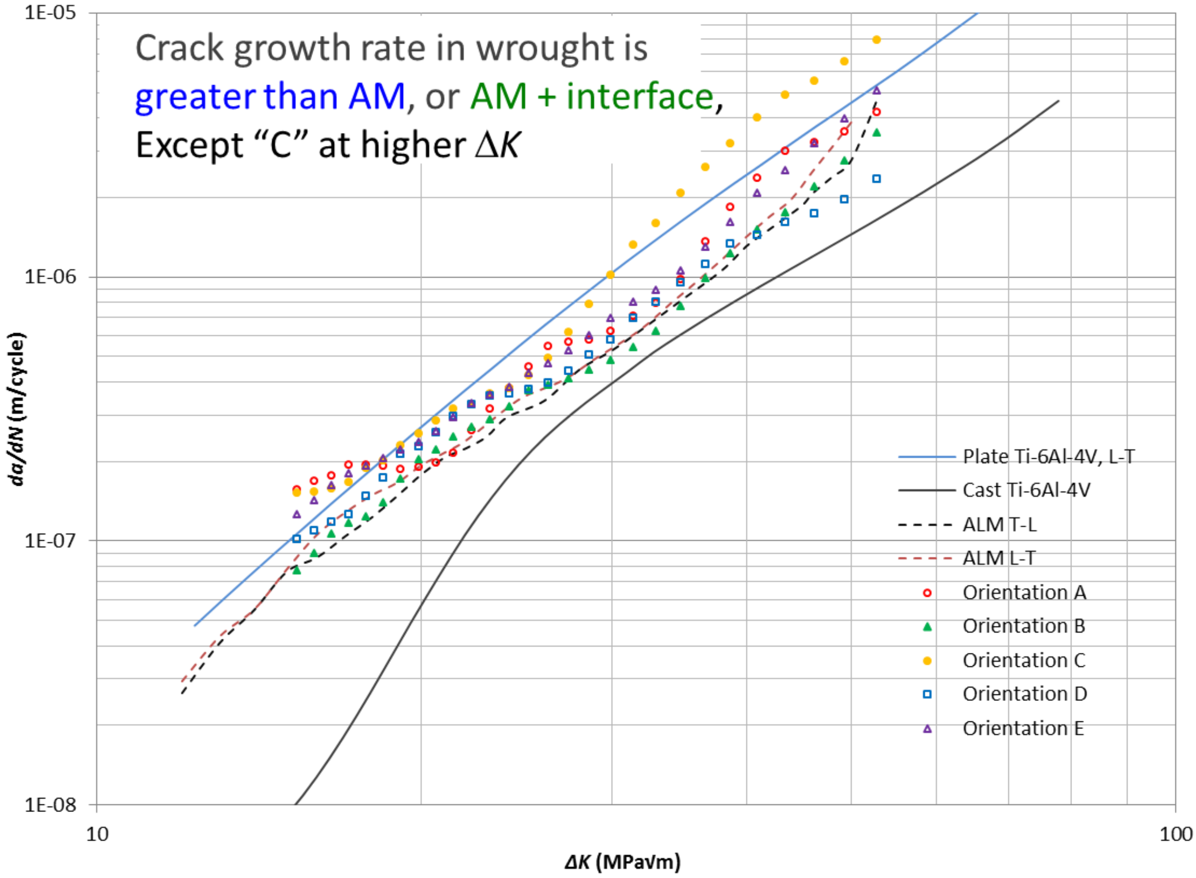

Figure 8. Summary of crack growth rate across WAAM to wrought interface in Ti-6Al-4V

Where the pre-crack is perpendicular to the interface, the crack grows in a linear manner across the interface at a rate which is representative of the material surrounding it. As shown in figure 9, when the pre-crack is at, or near the interface, it always propagates into, or toward the wrought material. Figure 9(a) shows the pre-crack at the interface, 9(b) shows the pre-crack on the WAAM side of the interface and figure 9(c) shows the pre-crack on the wrought side of the interface.

(a) Crack on the WAAM / wrought interface

(b) Crack on WAAM side of interface

(c) Crack on wrought side of interface

Figure 9. Crack propagation test samples with different pre-crack locations

2.6 The effect of cold rolling

As shown earlier, the properties of as-deposited titanium WAAM are mildly anisotropic. During work to investigate the use of cold rolling to reduce residual stress, a secondary effect was discovered (3). It was found that the cold rolling induced dislocations and strain energy into the crystal lattice of the material, which was released when the next layer was deposited. This caused a relaxation of residual stress, but also an apparent recrystallization of the material leading to a much refined grain structure with completely random grain orientations as shown in figure 10.

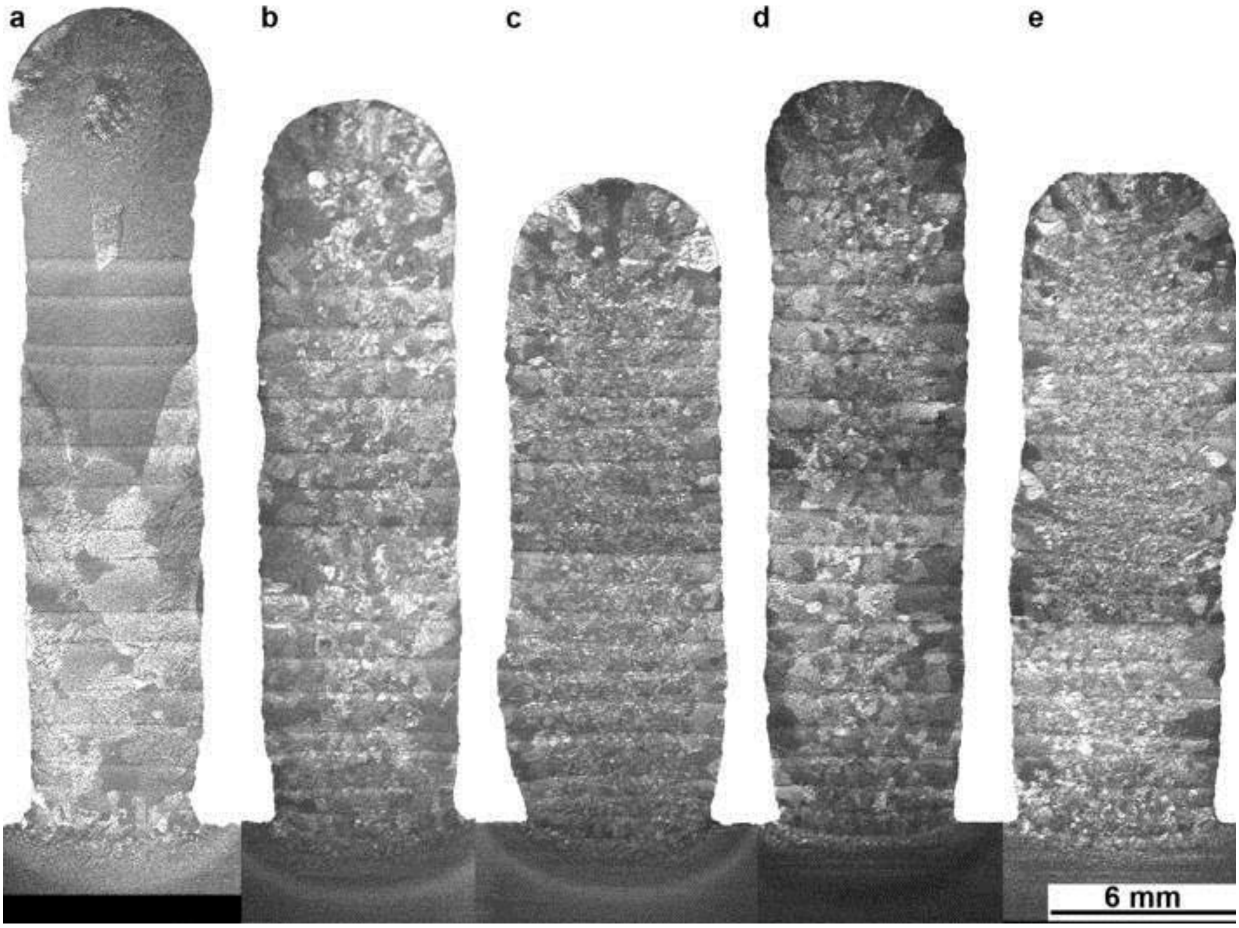

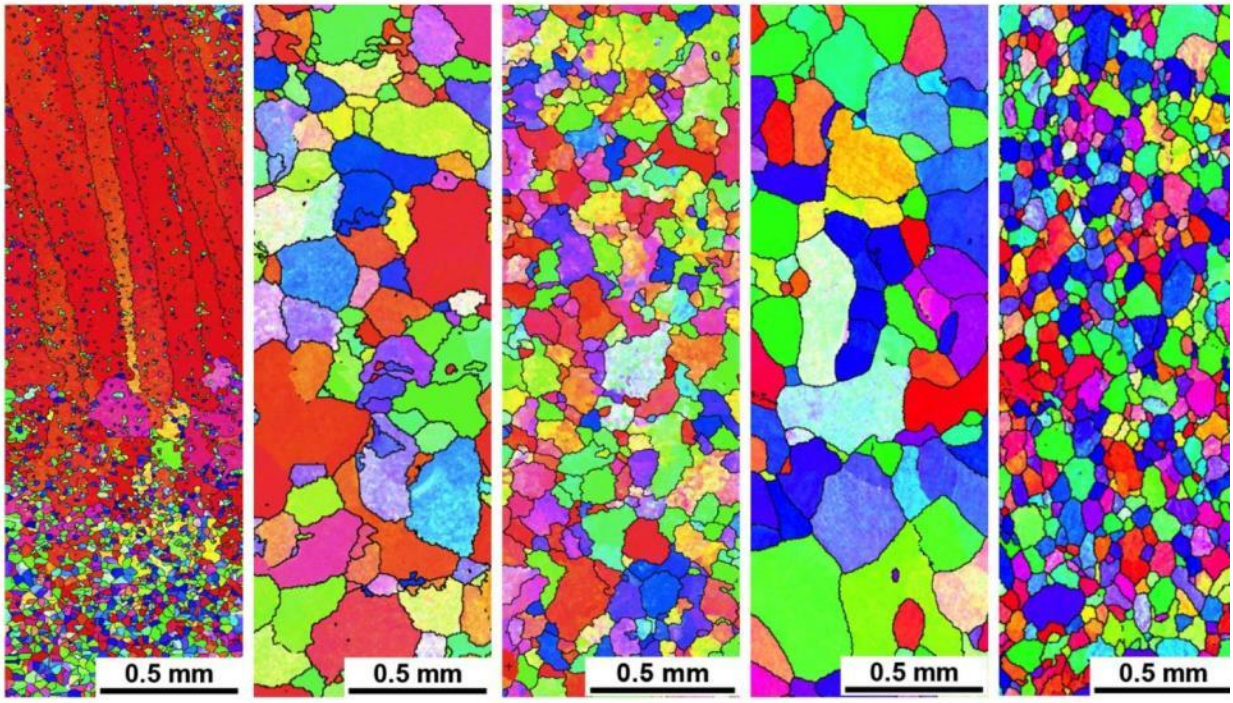

Figure 10. Metallographic sections and grain orientation images of control and rolled WAAM deposits

When tensile tests were performed on samples taken from rolled WAAM walls, it was found that the properties had both improved, and become isotropic as shown in table 1.

	Horizontal Reference	Horizontal Rolled	Vertical Reference	Vertical Rolled
2% Yield (MPa)	865	1020	805	995
UTS (MPa)	965	1075	918	1075
Elongation (%)	8.2	13	14.1	13

Table 1. Tensile properties of rolled Ti-6Al-4V WAAM deposit

3. Build of Complex parts with WAAM

3.1 Solid Model Preparation and build methodology

It should be remembered that WAAM is a near-net-shape manufacturing method and that in a similar manner to forging, a drawing or solid model of the required pre-form must be generated and it is this pre-form which is then considered for manufacture. The method by which the part will be built is considered, including placement of the substrate, separation of the part into discrete features and allocation of start stop points and feature build order. This process will to a great degree inform the adjustment of the net-shape part into a near-net-shape preform. The preparation of the near-net-shape model is a currently a manual process during which features such as large holes are closed, outer surfaces are shelled to give a final machining allowance, fillet radii and lead in and out structures are added to wall ends. Figure 11 gives an example of the difference between a net-shape and re-worked near-net-shape solid model.

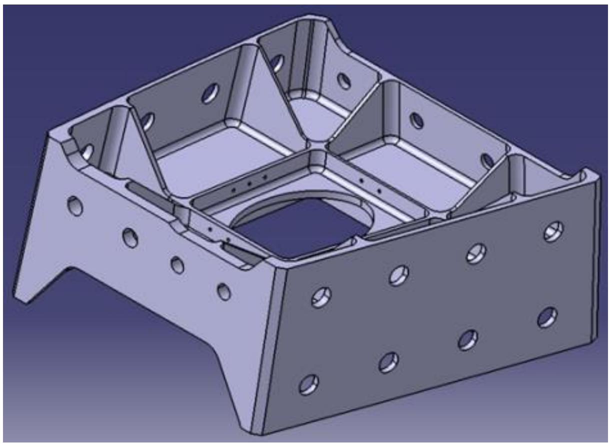

(a) Net Shape

(b) Re-worked near-net-shape

Figure 11. Example of solid model re-working for WAAM

Once the model is prepared, prototype software is used to slice it into layers and prepare path programmes for the WAAM system in use. The easiest and most common system is a revolute arm robot with integrated multi-axis positioner and deposition system. The part programme is downloaded into the system and tested to ensure there are no collisions between the deposition torch and jigs and fixtures. Deposition parameters are added and finally, the commitment to building a part is made.

The method described here is much simplified, with a great deal of skilled input currently required to correctly set variables such as layer height, feature build order, deposition parameters, cooling times and manipulation methods.

3.2 Examples of parts built using WAAM technology

3.2.1. Landing gear rib

A landing gear rib with a net-shape mass of 21kg from Bombardier Aerospace was examined and a demonstrator part built as shown in figure 12.

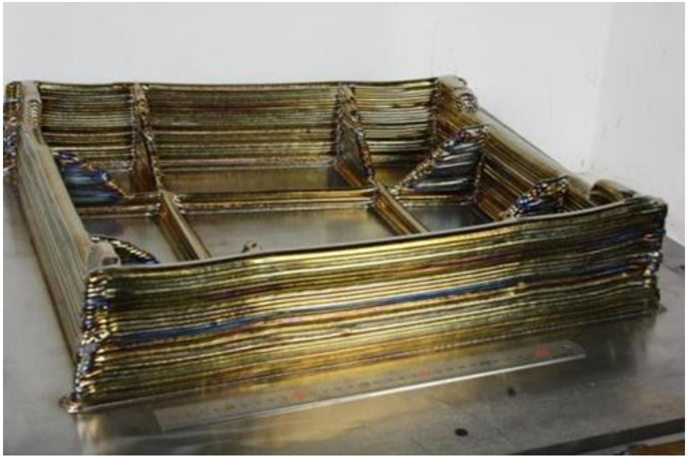

Figure 12. Landing gear rib demonstrator

The part took 24 hours to deposit, of which 30% was cooling time. The deposited part has a mass of 24kg and buy to fly ratio of 1.14:1, compared to machining from a billet of 240kg, with a buy to fly ratio of 11.5:1.

3.2.2 Frame Demonstrator

An assessment and build of the frame demonstrator shown in figure 14 was requested by BAE Systems. This part has some features which had not been encountered before, including a curved wall, varying wall thicknesses and wall interfaces at acute angles. Despite this, the part was successfully built at the second attempt.

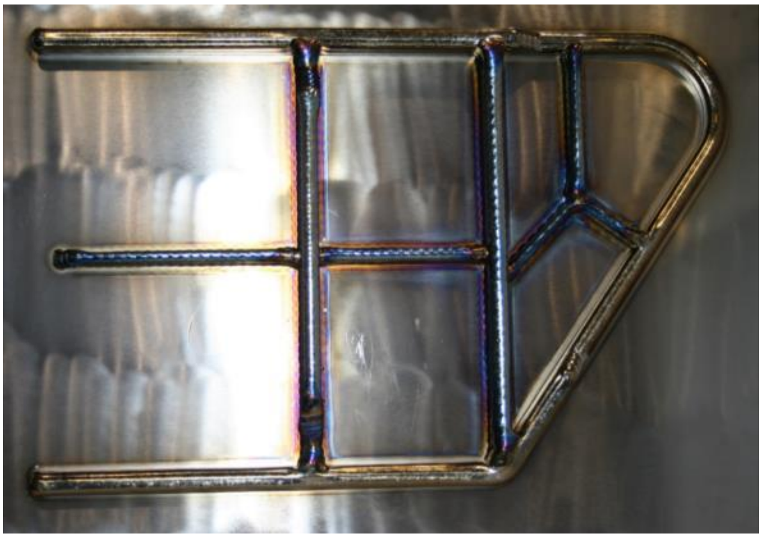

Figure 14. Frame demonstrator

The demonstrator has a deposited mass of 9kg, and took 11 hours to build.

3.2.3 Flap Rib Demonstrator

Fokker Aerostructures requested an assessment and build of a flap rib demonstrator part and shown in figure 15. This part presented some new challenges in tall, thin walls and several complex intersections. Development work was performed to reduce the minimum deposit width to 3.5mm and the part was built.

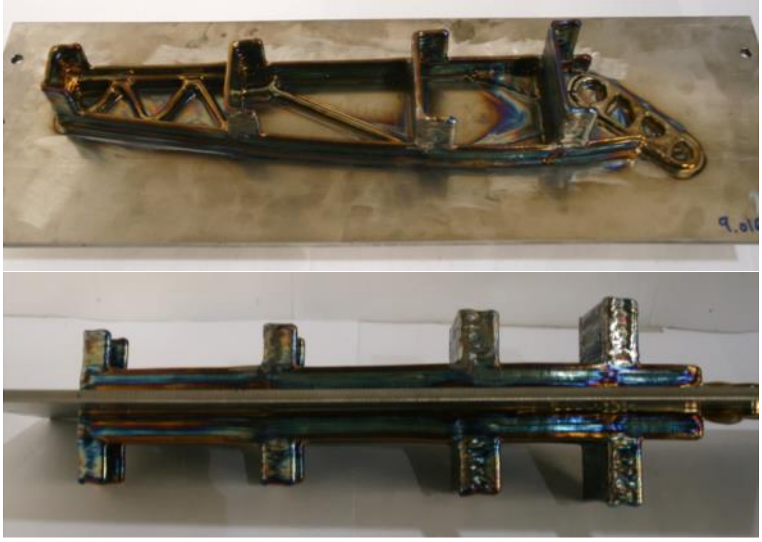

Figure 15. Two views of flap rib demonstrator part

Despite the difficulties of building thin walls, two versions of this part were built with the second built on a thinner substrate to improve the buy to fly ratio. The WAAM part took 9 hours to build, has a mass of 9kg and a buy to fly ratio of 6.3:1, compared to a billet mass of 53kg and buy to fly ratio of 37:1 to machine from solid.

3.2.4 High Complexity Demonstrator

A request to assess and build a high complexity additive manufacture demonstrator as shown in figure 16 was received from GKN Aerospace. As highlighted in the figure, this part contains several features which either had not been attempted before, or are known to be problematic for additive manufacturing processes and represents the most complex part build yet attempted at Cranfield University.

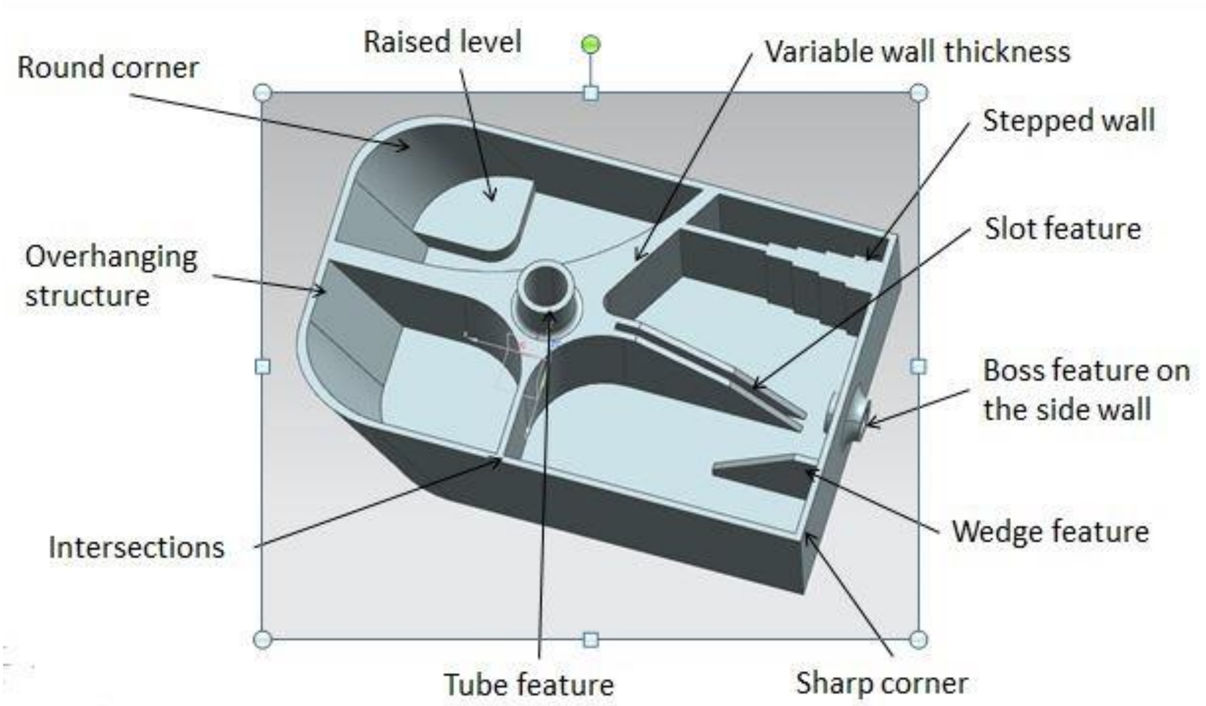

Figure 16. Illustration of high complexity demonstrator

The part was to be built in a symmetrical manner around a central substrate, requiring deposition of 40kg of material. In a slight change no normal, the wire was supplied on 600mm diameter spools, each containing just over 25kg. This reduced the material handling and environmental control requirements for the build considerably.

The part was successfully built as shown in figure 17, but there were several lessons learned during the build which led to interventions during manufacture, which would be incorporated in the part programme to improve subsequent builds. Unfortunately, due to project restrictions, it has not been possible to build a second, improved demonstrator. Detailed destructive examination of the first part has revealed some lack of fusion defects, which although unfortunate, were not entirely unexpected.

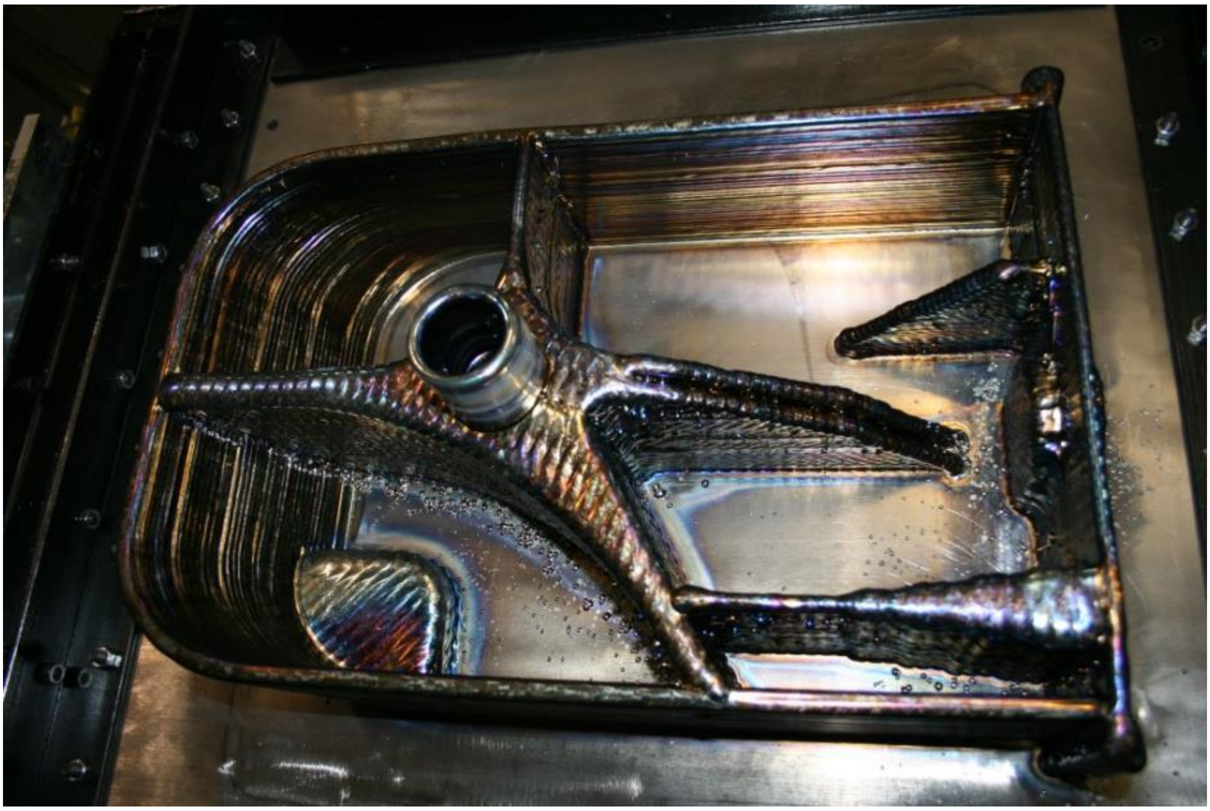

Figure 17. High complexity demonstrator part built by WAAM

Conclusion

As a process, WAAM has been shown to be capable of building relatively complex parts using readily available equipment without the need for expensive tooling and support structures. However, the interpretation, preparation and manufacture of parts is currently a highly skilled function for which only embryonic CAD/CAM software is available.

Parts which have been built to date clearly show it is possible to build with high material integrity and with good material properties in the as-deposited condition, which can be further improved by the inclusion of a cold working stage.

When considered against conventional manufacturing methods for the type of part under consideration, WAAM has also shown a potential to reduce overall material consumption, reduce reliance on large and expensive forgings, improve design flexibility because a fixed geometry forging is not required and to reduce the lead time for new, and replacement legacy parts.

Further work is required to develop CAD/CAM software support for WAAM, fully understand the mechanical properties of WAAM titanium alloy and to gain acceptance and qualification for parts made in this manner.

4. References

1. Wang, F., Williams, S., Colegrove, P., Antonysamy, A.A., 2013. Microstructure and Mechanical Properties of Wire and Arc Additive Manufactured Ti-6Al-4V. Metallurgical and Materials Transactions A 44, 968–977.
2. Martina, F., Mehnen, J., Williams, S.W., Colegrove, P., Wang, F., 2012. Investigation of the benefits of plasma deposition for the additive layer manufacture of Ti–6Al–4V. Journal of Materials Processing Tech. 212, 1377–1386.
3. Martina, F., Williams, S., Colegrove, P.A., 2013. Improved microstructure and increased mechanical properties of additive manufacture produced Ti-6Al-4V by interpass cold rolling, in: 24th International Solid Freeform Fabrication Symposium, Austin, Texas, USA. pp. 490–496.
4. Ding, J., Colegrove, P., Mehnen, J., Ganguly, S., Sequeira Almeida, P.M., Wang, F., Williams, S.W., 2011. Thermo-mechanical analysis of Wire and Arc Additive Layer Manufacturing process on large multi-layer parts. Computational Materials Science 50, 3315–3322.
5. Liu, S., 2015, The effect of oxygen content on the fracture toughness of additively manufactured Ti-6Al-4V, MSc Thesis, Cranfield University.
6. Hills, N., 2015, Fatigue Crack Propagation Behaviour at the Interface of Additively Manufactured Ti-6Al-4V and the Substrate, MSc Thesis, Cranfield University

Wire Plus Arc Additive Manufacture of Large Scale Titanium Parts

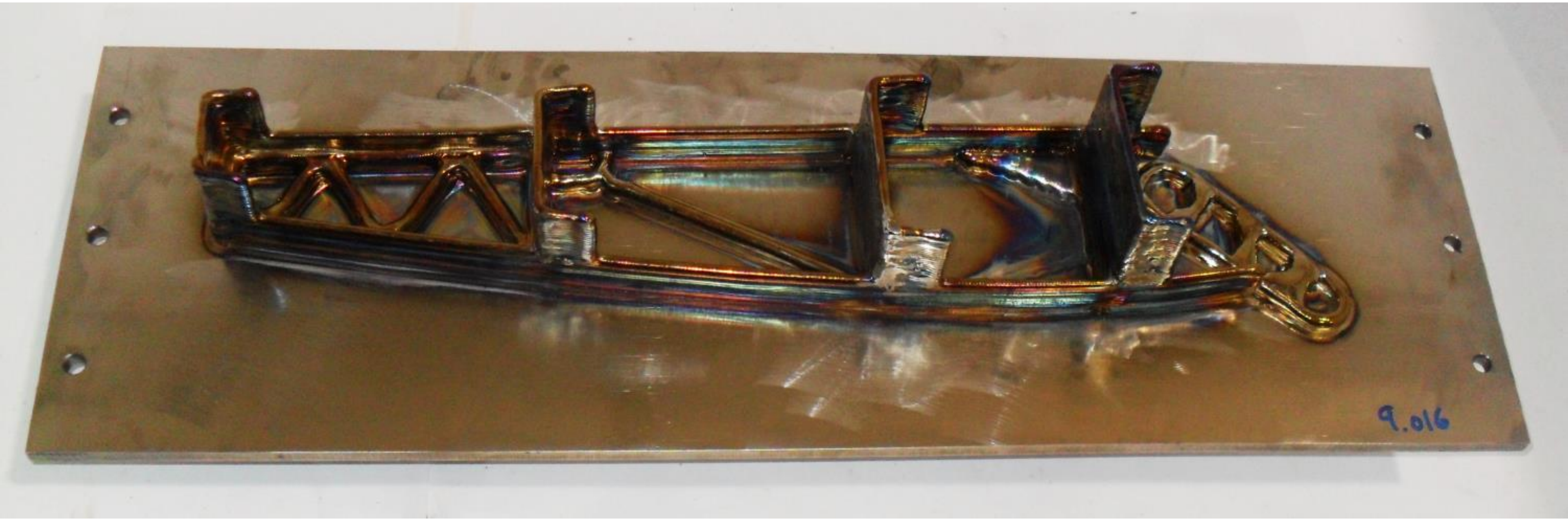

Adrian Addison + the WAAMMat team

Welding Engineering and Laser Processing Centre, Cranfield University

a.c.addison@cranfield.ac.uk

TITANIUM EUROPE2015
May 11-13 | Birmingham, UK

Presentation Contents

- Wire plus Arc Additive Manufacture
  - What is it and why use it?
- Mechanical Properties of Deposits
- Manufacture of complex parts
  - Landing Gear Rib
  - Frame Demonstrator
  - Flap rib demonstrator
  - High Complexity Demonstrator

WAAM Process

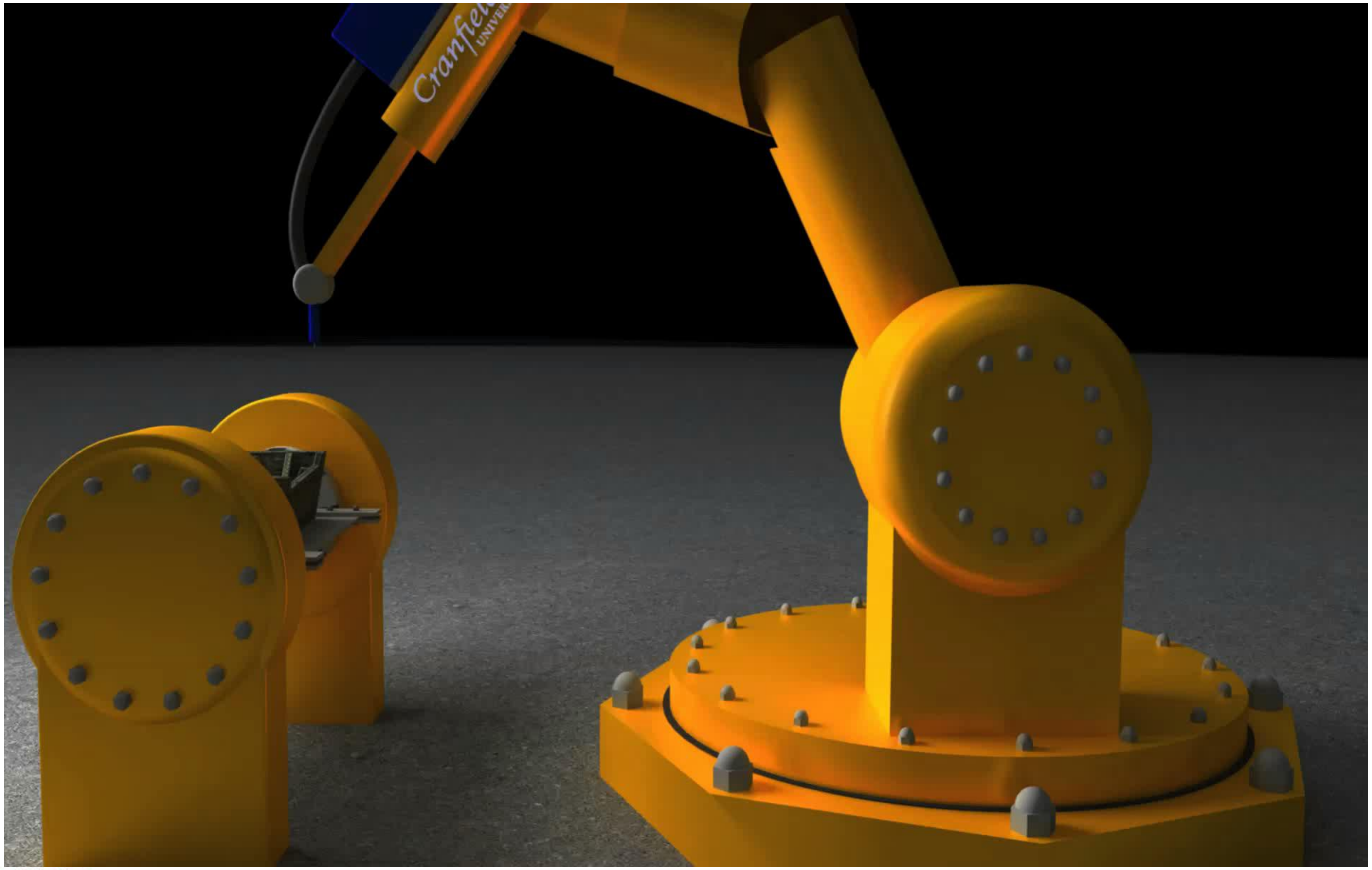

Cranfield UNIVERSITY

TITANIUM EUROPE2015 May 11-13 | Birmingham, UK

Why WAAM?

Complex structures?

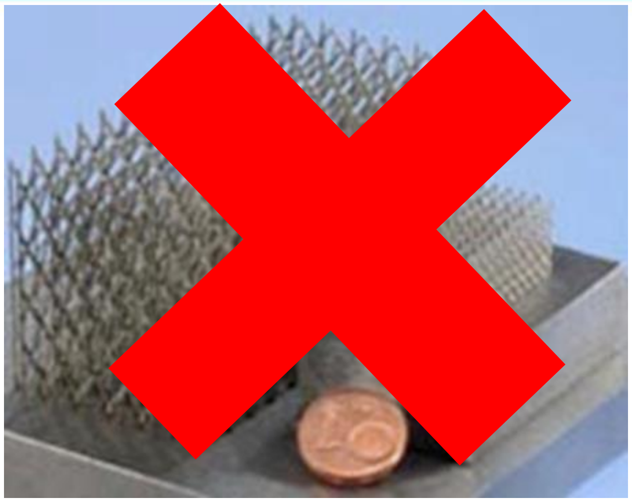

Design Freedom?

Metal Additive Manufacture - Business Drivers

Cranfield UNIVERSITY

WAAM advantages are:

Cost and material saving

Greatly reduced lead times

TITANIUM EUROPE2015 May 11-13 | Birmingham, UK

Ti 6Al 4V Mechanical properties summary

	Yield Strength (MPa)	Ultimate Strength (MPa)	Elongation (%)
Specification minima*	824	896	6.0
Wrought Ti64	950	1034	11.7
WAALM Vertical	805	918	14.1
WAALM Horizontal	865	965	8.2

*AMS 4985 Cast and HIP

Ti 6Al 4V as deposited fatigue

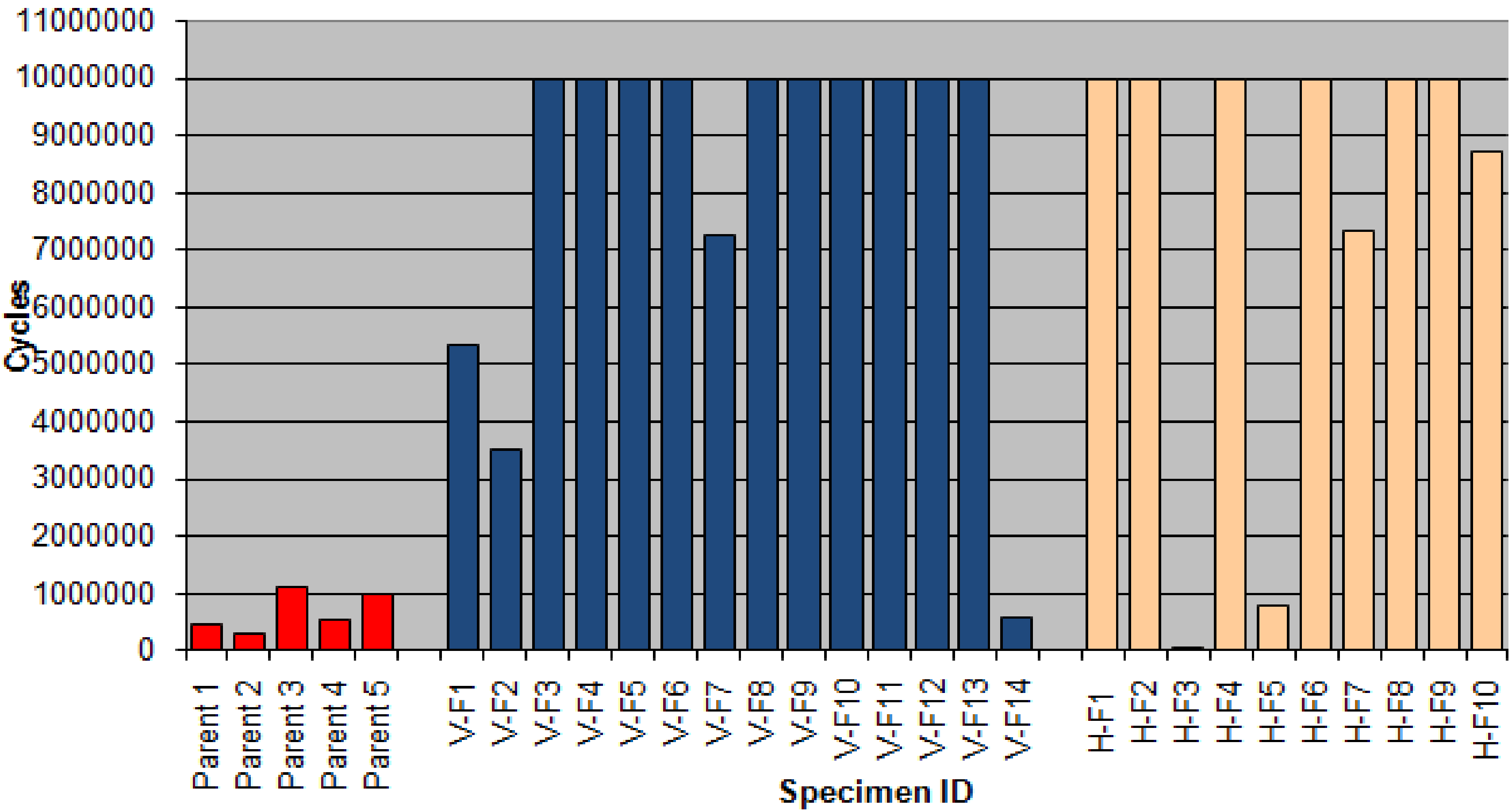

R-Ratio 0.1, σ_{max}=600MPa, Sinusoidal Waveform and 30Hz,

Fracture Toughness K_{IC} (thickness = 19 mm)

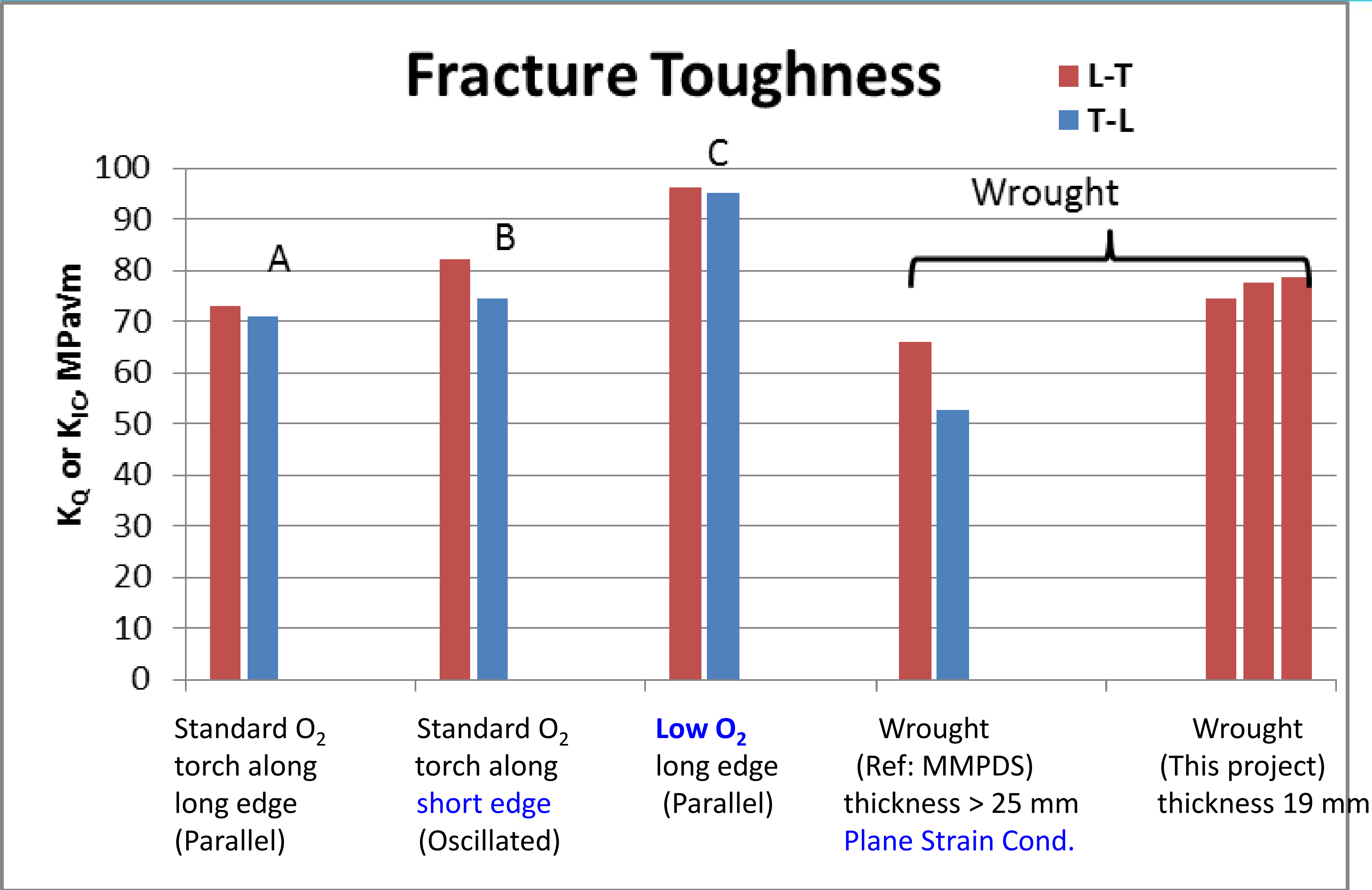

Fatigue crack growth rate

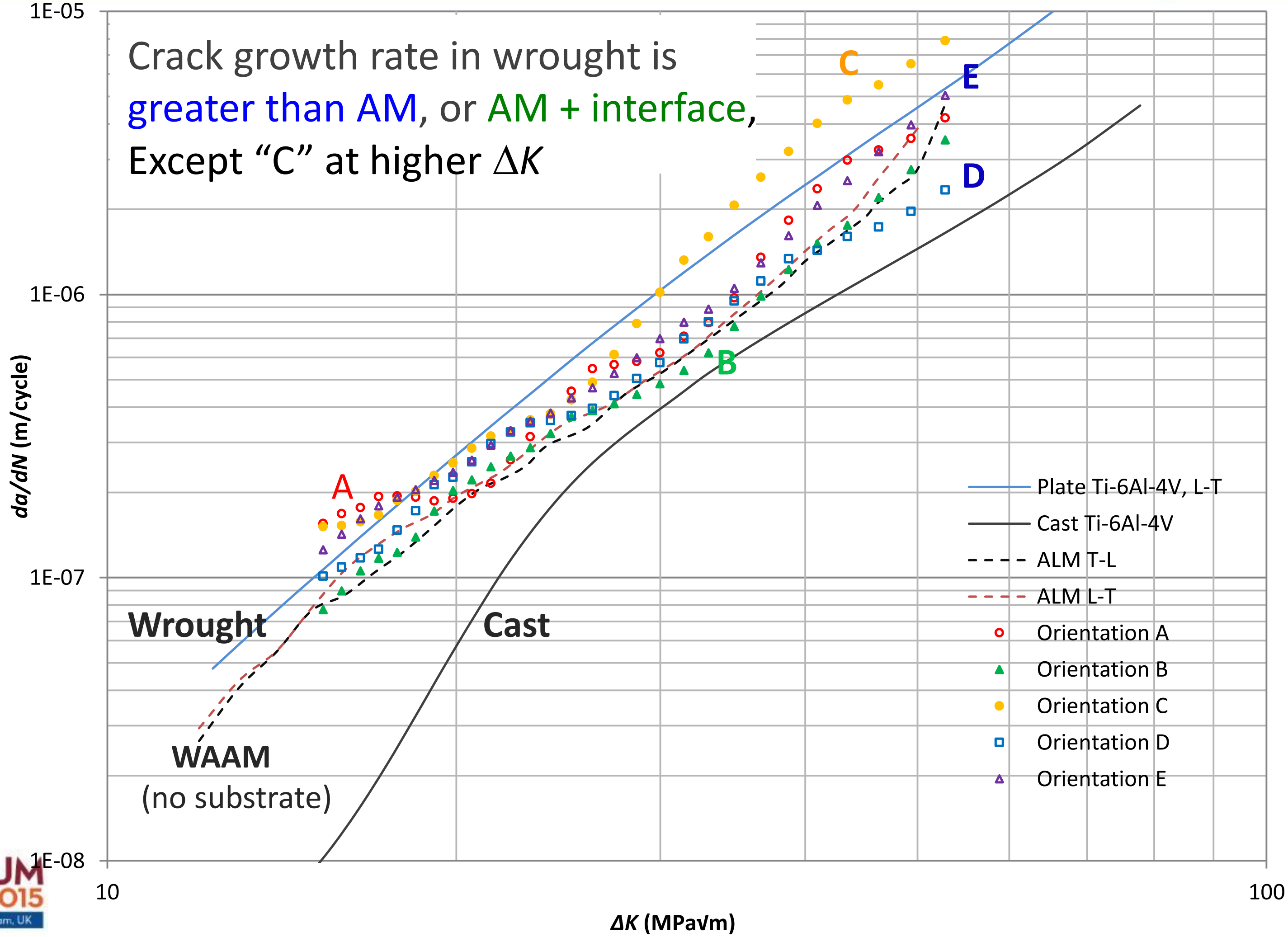

Rolling of AM parts // How it works

Cranfield UNIVERSITY

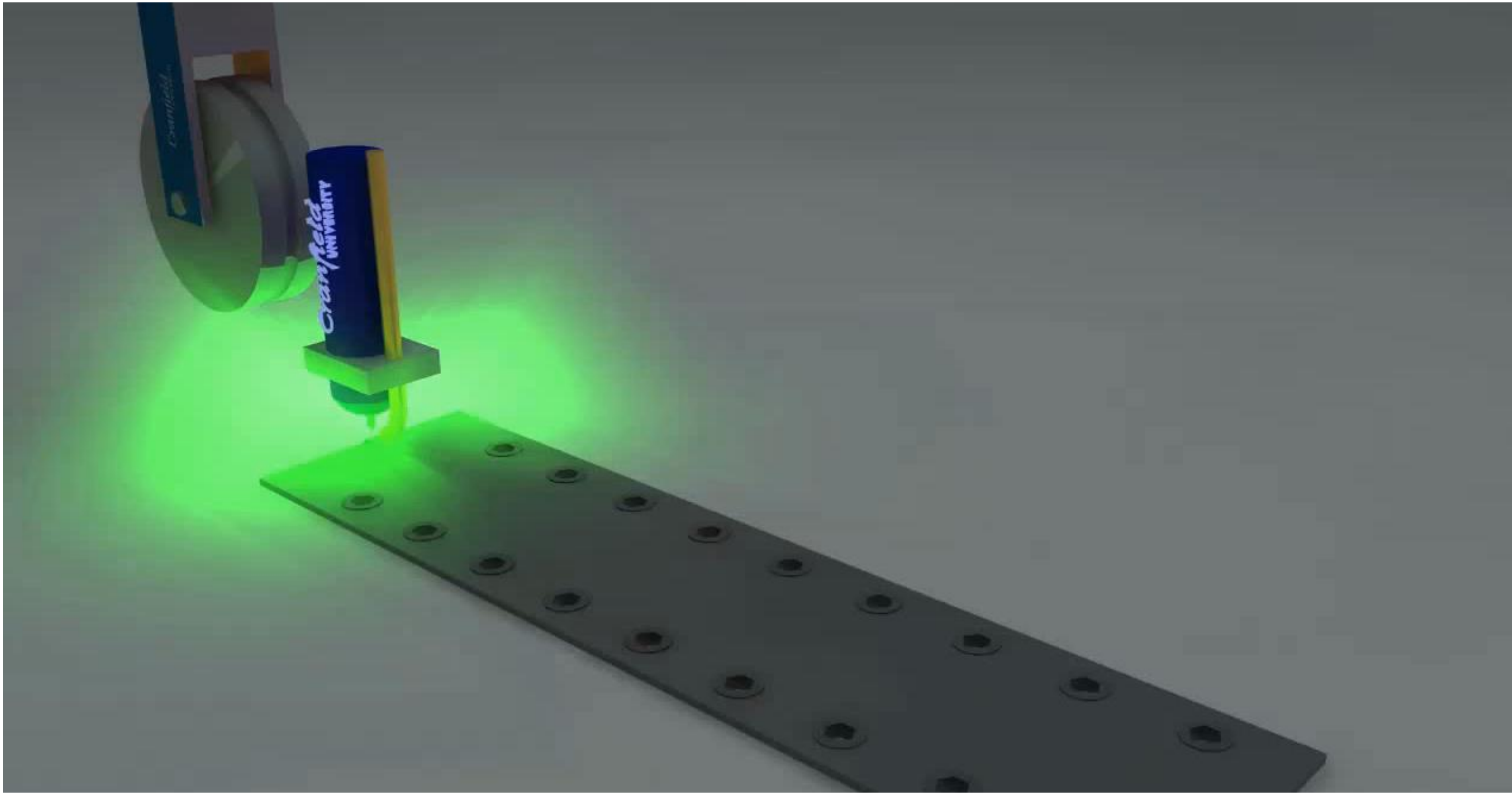

Guaranteeing mechanical properties by Rolling

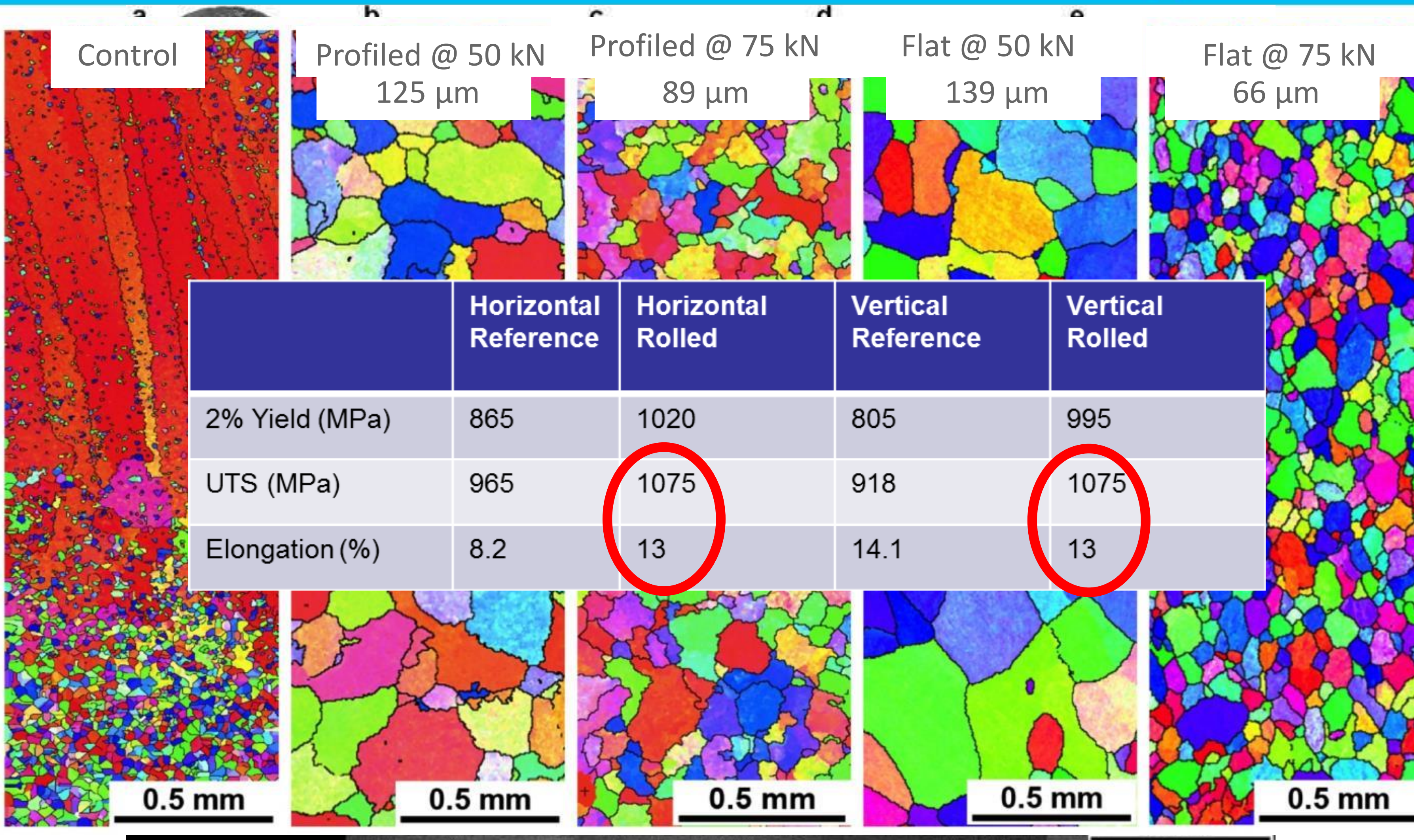

	Horizontal Reference	Horizontal Rolled	Vertical Reference	Vertical Rolled
2% Yield (MPa)	865	1020	805	995
UTS (MPa)	965	1075	918	1075
Elongation (%)	8.2	13	14.1	13

WAAM - Example parts - Landing gear rib for Bombardier Aerospace

Cranfield UNIVERSITY

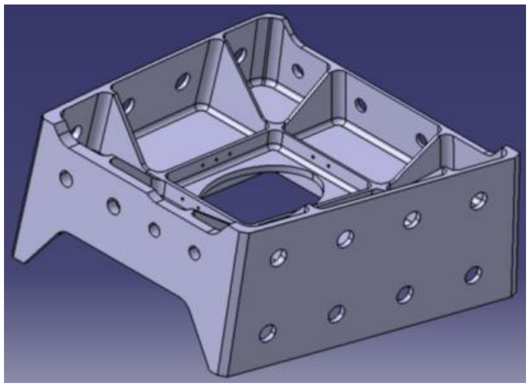

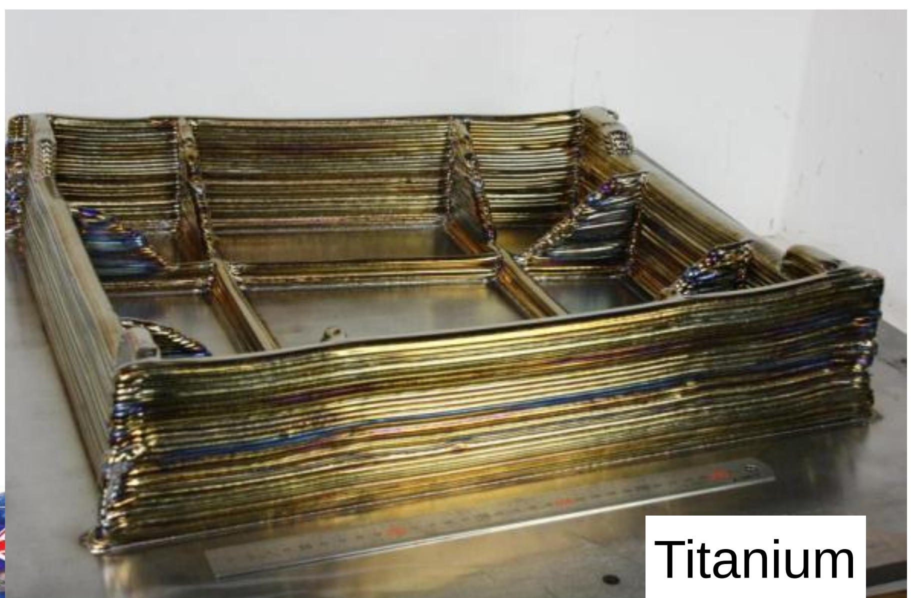

	Before (kg)	After (kg)	Buy-to-fly	Waste
Machining	240	21	11.6	91%
AM	24	21	1.15	13%

Deposition time - 24 hours

WAAM - Example parts - Landing gear rib version 2

Cranfield UNIVERSITY

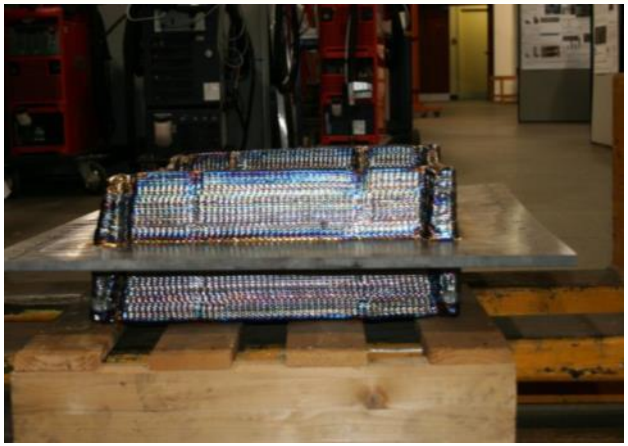

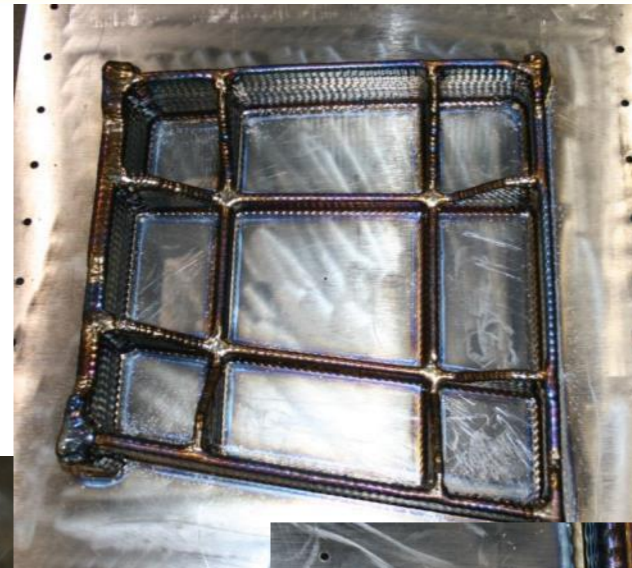

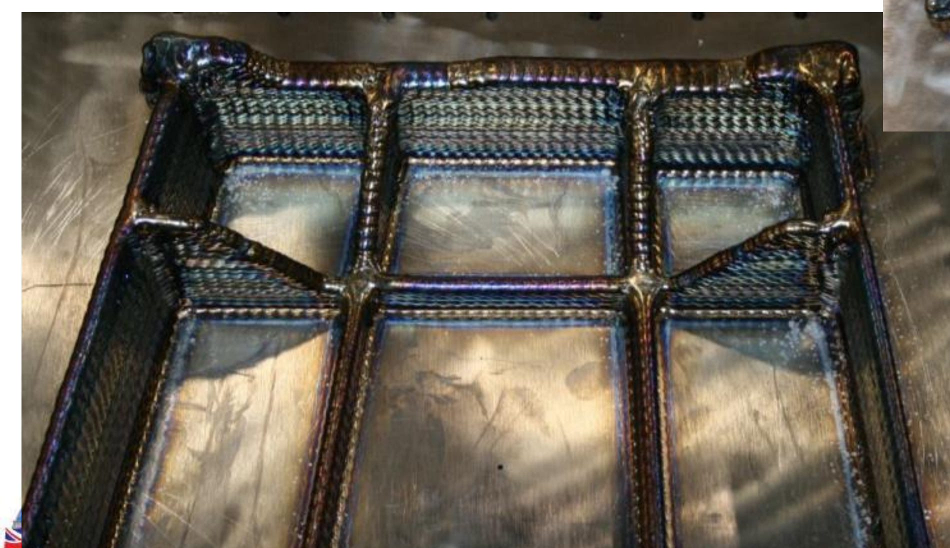

Frame Demonstrator for BAE Systems

Cranfield UNIVERSITY

Main features

- Round corner
- Intersections
- Varying wall width
- Double sided

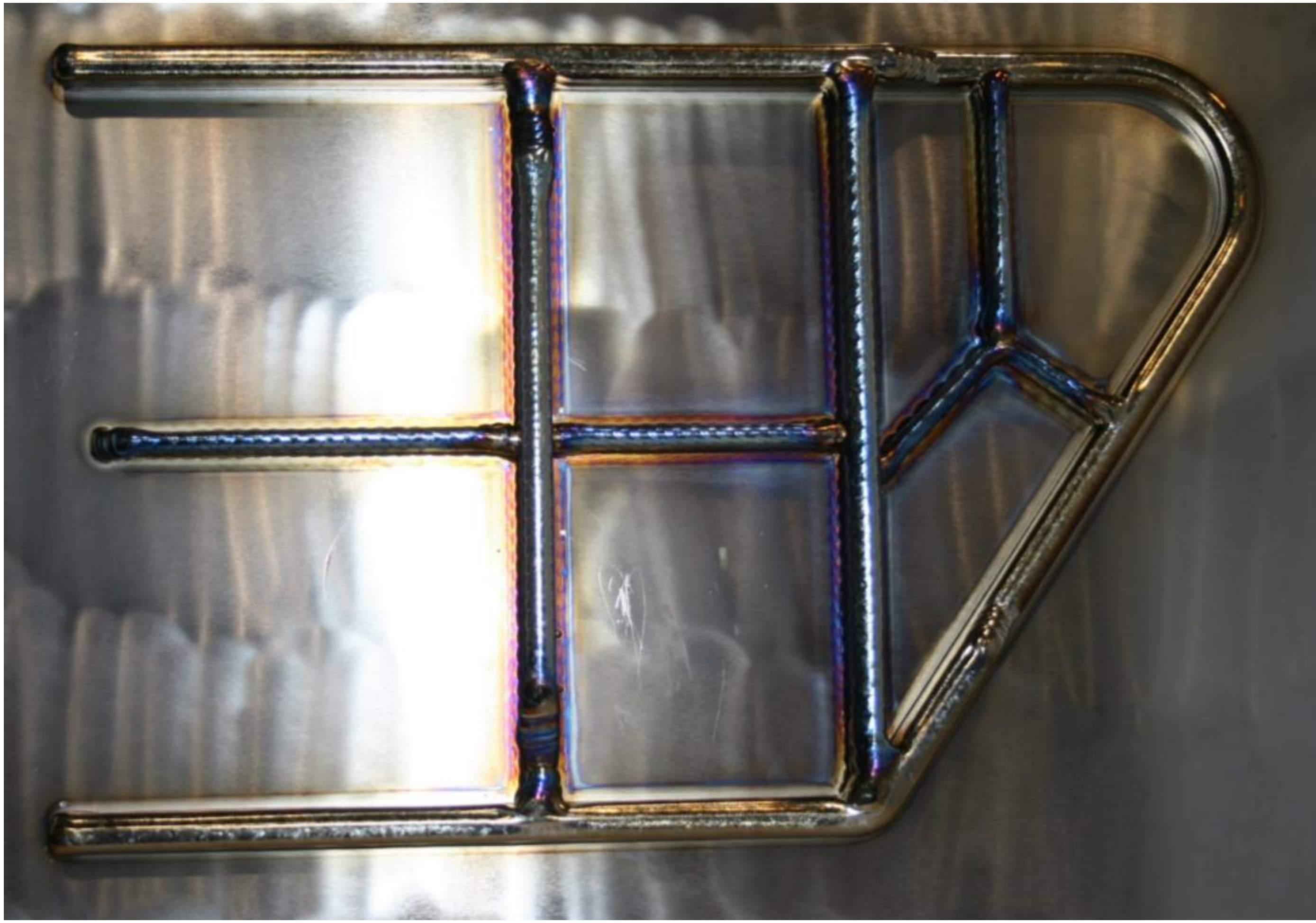

TITANIUM EUROPE2015
May 11-13 | Birmingham, UK

Cranfield UNIVERSITY

Frame Demonstrator

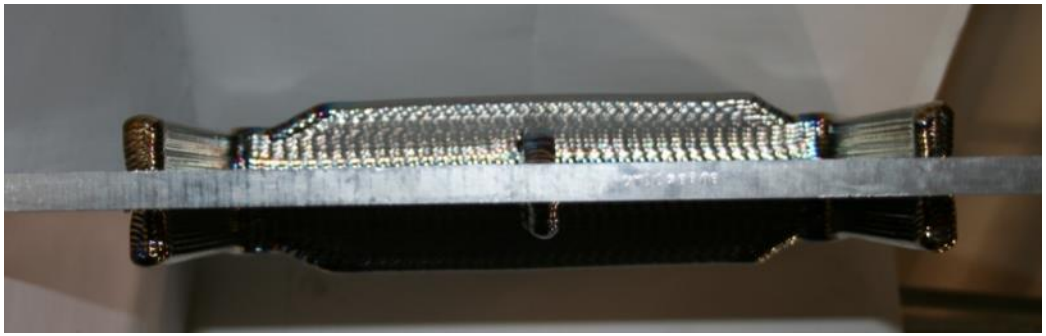

Double sided symmetrical structure controls distortion

Oscillated inner walls allow fillet radii

Parallel bead outer walls simplify intersections and circular features

Flap Rib Demonstrator for Fokker Aerostructures

Cranfield UNIVERSITY

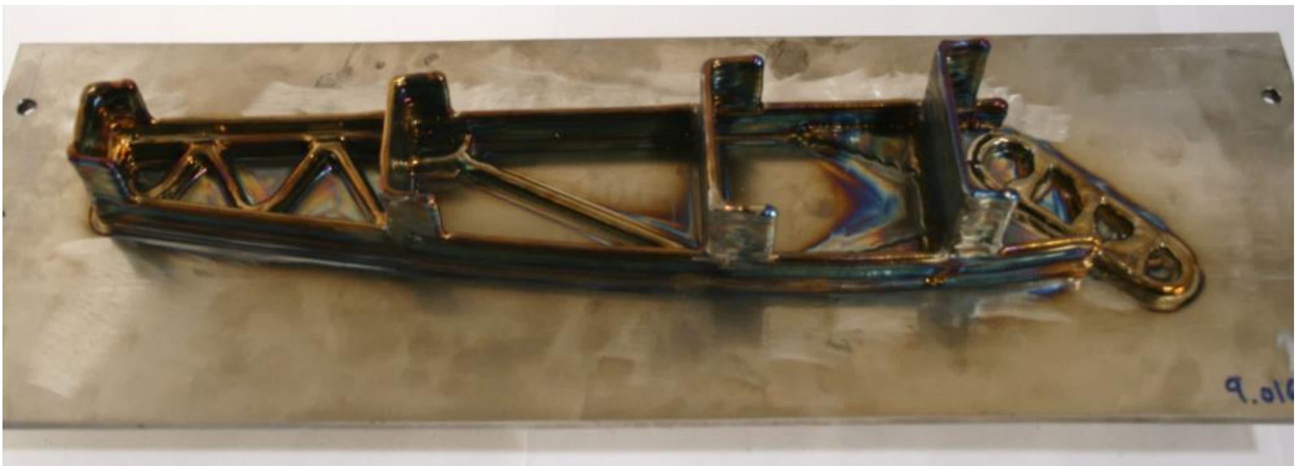

- Building time: 2 days
- Minimum Wall thickness: 4.4 mm
- Weight as design: 1.43 kg
- Billet weight 53kg
    - BTF = 37:1
- Weight as deposited (with plate): 9.0 kg
    - BTF: 6.3:1
- Further optimisation possible

High Complexity Demonstrator for GKN Aerospace

Cranfield UNIVERSITY

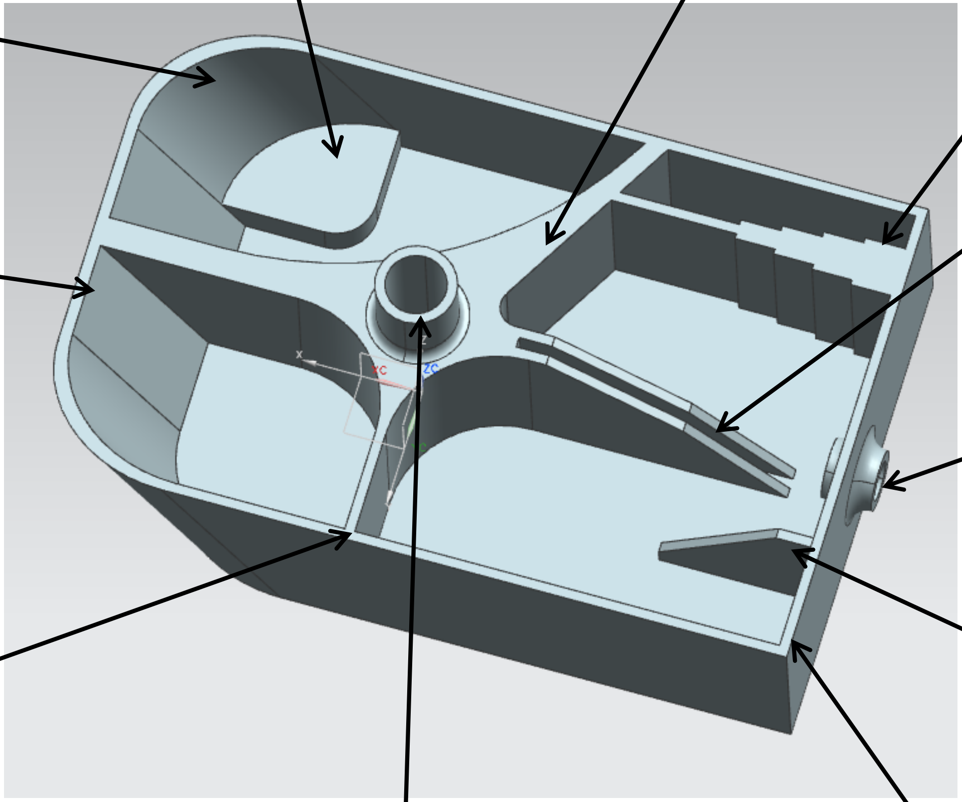

TITANIUM EUROPE2015 May 11-13 | Birmingham, UK

High Complexity Demonstrator

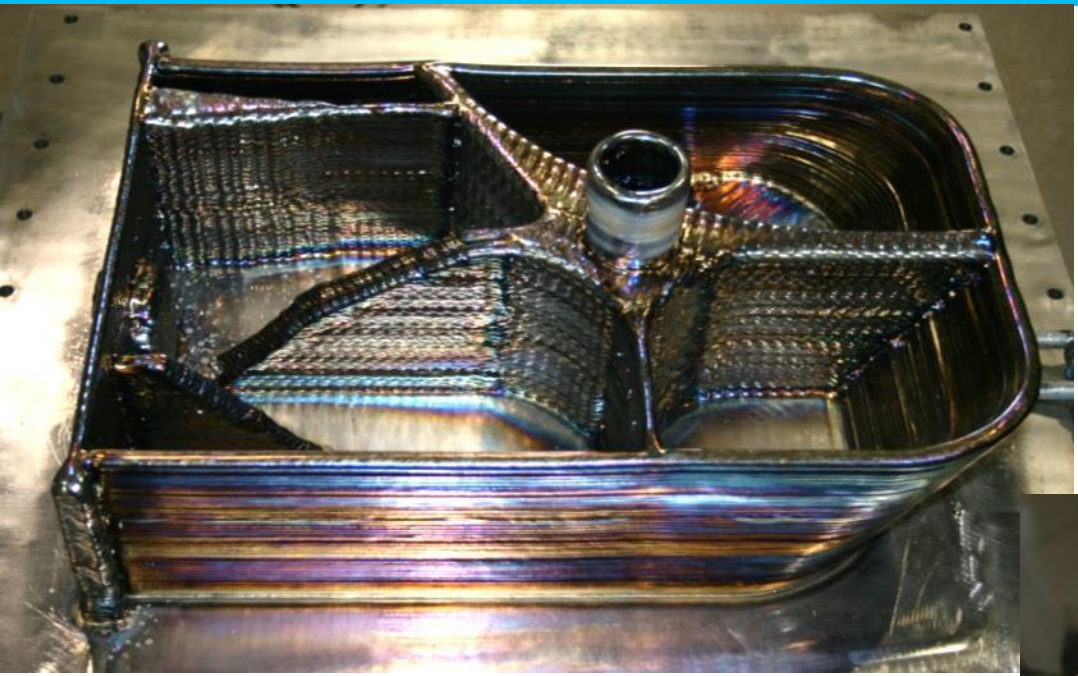

Hardware improvement: large Ti-6Al-4V spools (25 kg each)

Deposition rate:

- Outside wall parallel beads: 2.0m/min (0.65kg/hour)
- Inside wall oscillated beads: up to 3.8 m/min (1.25kg/hour)

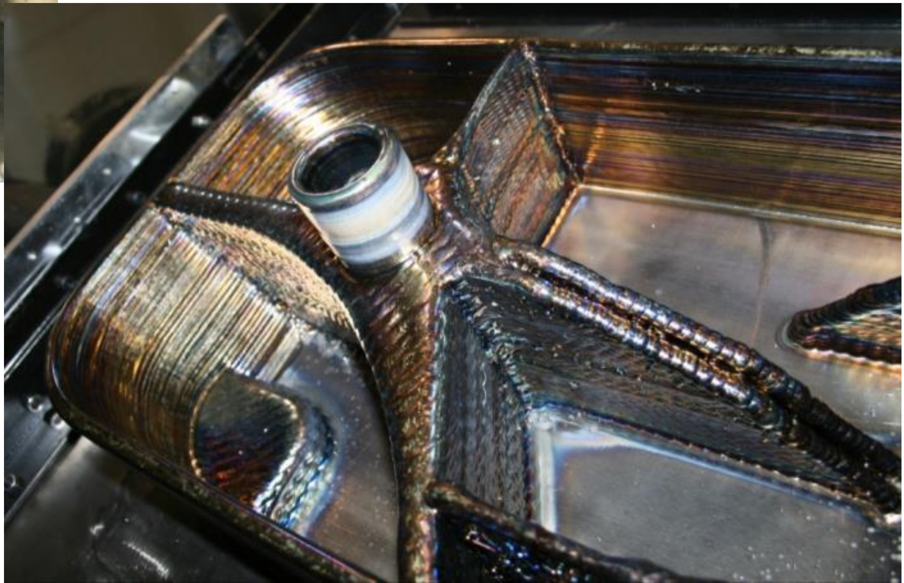

Mass: ~40kg.

BTF: 1.3

Building time: two weeks

To whom the credit is due…

Professor Stewart Williams - s.williams@cranfield.ac.uk
Dr Paul Colegrove - p.colegrove@cranfield.ac.uk
Dr Jialuo Ding - jialuo.ding@cranfield.ac.uk
Dr Helen Lockett - H.Lockett@cranfield.ac.uk
Filomeno Martina - f.martina@cranfield.ac.uk
Jianglong Gu - jianglong.gu@cranfield.ac.uk
Dr Xiang Zhang - Xiang.Zhang@cranfield.ac.uk
Goncalo Rodrigues Pardal - g.n.rodriguespardal@cranfield.ac.uk
Sonia Martins Meco - s.a.martinsmeco@cranfield.ac.uk
Sergio Rios Contesse - s.e.rioscontesse@cranfield.ac.uk
Yuehai Feng - yuehai.feng@cranfield.ac.uk
Flemming Nielsen - f.nielsen@cranfield.ac.uk
Brian Brooks - b.brooks@cranfield.ac.uk

Cranfield UNIVERSITY

Thank you for listening

Any Questions?

a.c.addison@cranfield.ac.uk
www.cranfield.ac.uk